PHILOSOPHICAL TRANSACTIONS OF THE ROYAL SOCIETY A MATHEMATICAL, PHYSICAL & ENGINEERING SCIENCES

A Study of a High-Current Toroidal Ring Discharge

A. A. Ware

Phil. Trans. R. Soc. Lond. A 1951 **243**, 197-220
doi: 10.1098/rsta.1951.0002

A STUDY OF A HIGH-CURRENT TOROIDAL RING DISCHARGE*

By A. A. WARE, Ph.D.
Imperial College of Science and Technology

(*Communicated by Sir George Thomson, F.R.S.—Received* 22 *May* 1950—
Revised 29 *July* 1950)

[Plates 2 and 3]

CONTENTS

A toroidal ring discharge has been studied in which the exciting primary is a metal coating on the outside of the torus. The waveforms of the currents and electric fields in the gas have been obtained, and the light from the discharge has been studied spectroscopically and with a photo-multiplier, the gases used being hydrogen and argon. Very large currents flow in the gas with peak amplitudes greater than 10^4 A. The current is in phase with the electric field, the exciting frequency being 150 kc./sec. Photographs of the discharge show a marked 'pinch' effect in argon. The method of Craggs & Hopwood (1947) has been applied to determine the ion concentrations from the broadening of the Balmer lines. Peak ion concentrations occur which are greater than the molecular concentrations. High-frequency oscillations (1 to 5 Mc./sec.) occur in the gas and are thought to be plasma ion oscillations.

1. Introduction

Although frequently used as a light source in spectroscopy, the ring discharge has not been widely studied. Sir J. J. Thomson (1927, 1928) demonstrated that the circulating currents were of the same order of magnitude as those in the exciting coil and estimated that the ion concentrations were comparable with the number of molecules per cm.^{3} when the gas pressure was 10^{-2} mm. Hg. Knipp & Knipp (1931) were able to obtain a direct reading of the current in a ring discharge but only at the expense of greatly modifying the simple circular ring discharge. That the gaseous currents could be deduced from the increase in frequency caused by a ring discharge was shown by Tykocinski-Tykociner (1932) and Kunz (1932),

* This work has been approved by the University of London for the award of the degree of Ph.D.

but the experimental work of the former was spoilt by a longitudinal discharge occurring in his discharge tube. Esclangon (1934) measured the power dissipated in a ring discharge and deduced the gas current by applying the theory of the induction furnace. When the amplitude of the electric field was 4 V/cm. the circulating current was 10 A.

The only recent work on the ring discharge has been done by Smith (1941, 1947), who studied a form of ring discharge in which the magnetic field linked but did not invade the gas. Using a very low frequency (900 c./sec.) an intense discharge of 400 A peak current was obtained in mercury vapour at 10^{-4} mm. Hg, although the voltage per turn of the exciting coil was only 7 V. The induced currents were measured by using two balanced measuring coils, one of which was coupled with the gas more than the other. When a current passed in the gas the excess flux linking one coil produced a current in the measuring circuit proportional to the current in the gas. The absolute magnitude of the current was obtained from consideration of the power expended in the gas. Probe measurements showed that the gas was about 13 % ionized and the electron temperature 10^5 °K.

Recently a type of ring discharge has been suggested by Steenbeck as a form of induction accelerator. The discharge vessel consists of a toroidal tube which is coated with metal on the outside except for a small gap at one point of the circumference. A ring discharge is produced within the torus by discharging a bank of condensers through the metal coating which acts as a single-turn coil tightly coupled with the gas inside it. Steenbeck suggested that because the cross-section of gas atoms decreases with increase in electron velocity, it should be possible for there to exist in the discharge a group of fast electrons which would behave as if they were in a vacuum. He also claimed that the magnetic fields within the torus would be such as to focus and guide these electrons so that the discharge would behave as an induction accelerator similar to the betatron. The main body of the discharge would be maintained by slow electrons with normal free paths. Preliminary studies with such an apparatus were made by Steenbeck towards the end of the war. No papers have been published on the 'Wirbelrohr' (Steenbeck's name for this accelerator), and the only information available is a report made by T. Wasserrab to the British authorities.* A summary of this report has been issued from Harwell (1946).

The work to be described here was aimed at studying the physical properties of this special type of ring discharge suggested by Steenbeck.

2. Description of apparatus

Discharge tube

The form of discharge tube used in most of the experimental work is shown in figure 1. It consisted of a glass torus which was made by bending 3 cm. diameter Pyrex tubing into

* *Note added in proof.* Since this paper was submitted for publication it has been brought to the author's notice that Steenbeck did publish a paper on the 'Wirbelrohr'. This paper (Steenbeck & Hoffmann, 1943) describes some preliminary experiments which were carried out with a discharge tube similar to that described above. Oscillograms were taken of voltages connected with the discharge circuit and the gas current waveforms were deduced graphically. These waveforms are similar to those described above. Peak gas currents of 10,000 A are recorded, the capacity used being 15 μF and the voltage 10 kV. In particular Steenbeck & Hoffmann noted the long formative time lags which occur in the breakdown at low pressures. A search was made for X-rays and at the lowest gas pressures (0·03 mm. Hg) a faint darkening of photographic film was obtained.

a circle of diameter 25 cm. The tube was coated on the outside with copper which was about a hundredth of an inch thick, a gap (G) about 1·8 cm. wide being left at one point of the circumference. On the opposite side of the torus to G an inspection window (W) was constructed by sealing to the torus a short length of glass tubing of slightly greater diameter than the discharge tube, the tubing being parallel to the axis of the torus. The other end of this tube was sealed with a circular piece of plane Pyrex glass. The discharge tube had two side-arms at opposite ends of a diameter by means of which the torus was connected to the vacuum system. The electrical connexions to the torus were made by means of two copper straps which were wrapped around the copper coating on either side of the gap G. (The gap G is referred to later as the 'feed-point gap')

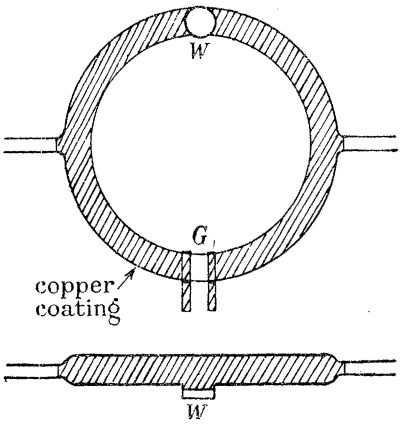

FIGURE 1. The discharge tube.

The gases studied in the discharge were hydrogen and argon which were of commercial purity.

The condensers and electrical circuit

The condenser bank used in the work described here consisted of four 0·5 μF condensers, capable of working at 25 kV, connected in parallel. The discharge circuit consisted simply of the metal coating of the torus connected by the shortest possible leads to the condensers with a switching device in one lead. The switch consisted of a three-electrode spark gap of the type developed by Craggs, Haine & Meek (1946). The particular form used was one in which the electrodes were adjustable and open to the atmosphere. The electrodes were mounted in a box of insulating material which had several ventilation holes. The spark gap was fired by applying a short high-voltage pulse to the trigger electrode.

The position of the torus with respect to the condensers is shown in figure 2. The four condensers (C) were placed in the form of a square with their terminals pointing upwards. The torus was mounted in a vertical plane just above the condensers, and the leads from the condensers to the torus and the spark gap (S) were as shown. Separate leads from each condenser were used so as to keep the inductance of the circuit down to a minimum. With this arrangement the resonant frequency was 143 kc./sec., the total inductance being 0·65 μH. Just less than half the condenser voltage was developed across the torus.

The cathode-ray oscilloscope

The oscilloscope used incorporated a G.E.C. cathode-ray tube which has a blue fluorescent screen and an anode potential of 4000 V. The oscillograms were photographed by means of

a Cossor oscilloscope camera, and with the above tube and Kodak's most sensitive recording film (R 60) it was found possible to photograph a single sweep of the oscillogram, the duration of which was about 20 μsec. The time-base circuit used was of standard design.

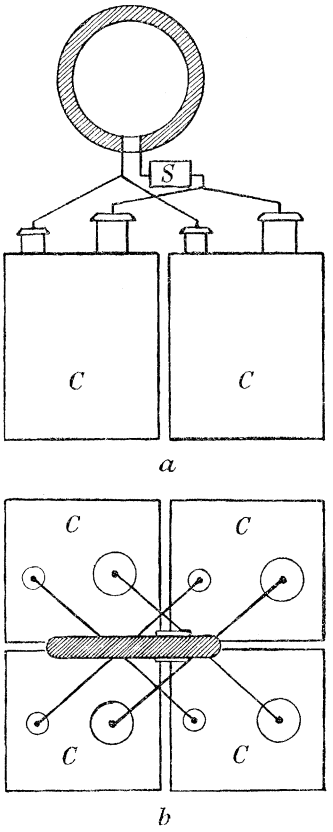

FIGURE 2. The position of the torus: *a*, elevation; *b*, plan.

Photo-multiplier circuit

The light emitted from the discharge was studied with a type 931 A photo-multiplier tube. So as to obtain a good frequency response the load resistance in the anode circuit was kept small in value and an amplifier used so as to give an output of sufficient amplitude to be observed on the oscilloscope. The upper frequency limit of the amplifier was about 1·5 Mc./sec.

Because of the brightness of the discharge it was found necessary to restrict severely the amount of light reaching the photo-multiplier so as to prevent saturation. An image of the part of the discharge under study was thrown on to a narrow slit in front of the photo-multiplier. By adjusting the slit the amount of light reaching the sensitive cathode could be controlled over a wide range. The output from the amplifier was observed on the oscilloscope.

3. GENERAL DESCRIPTION OF THE DISCHARGE

The ranges of pressures for which a discharge will occur in hydrogen and argon can be seen from figure 3, which shows the breakdown voltage plotted against pressure. The left-hand axis gives the minimum voltage to which the condensers must be charged so as to produce a visible discharge in the gas. At medium and low pressures the onset of a discharge was clearly marked. Nothing was observed until a definite voltage was reached, whereupon

a very bright discharge occurred. At high pressures however, the onset was not clearly defined; a visible discharge gradually appeared as the voltage was increased, being very faint at first and slowly getting brighter.

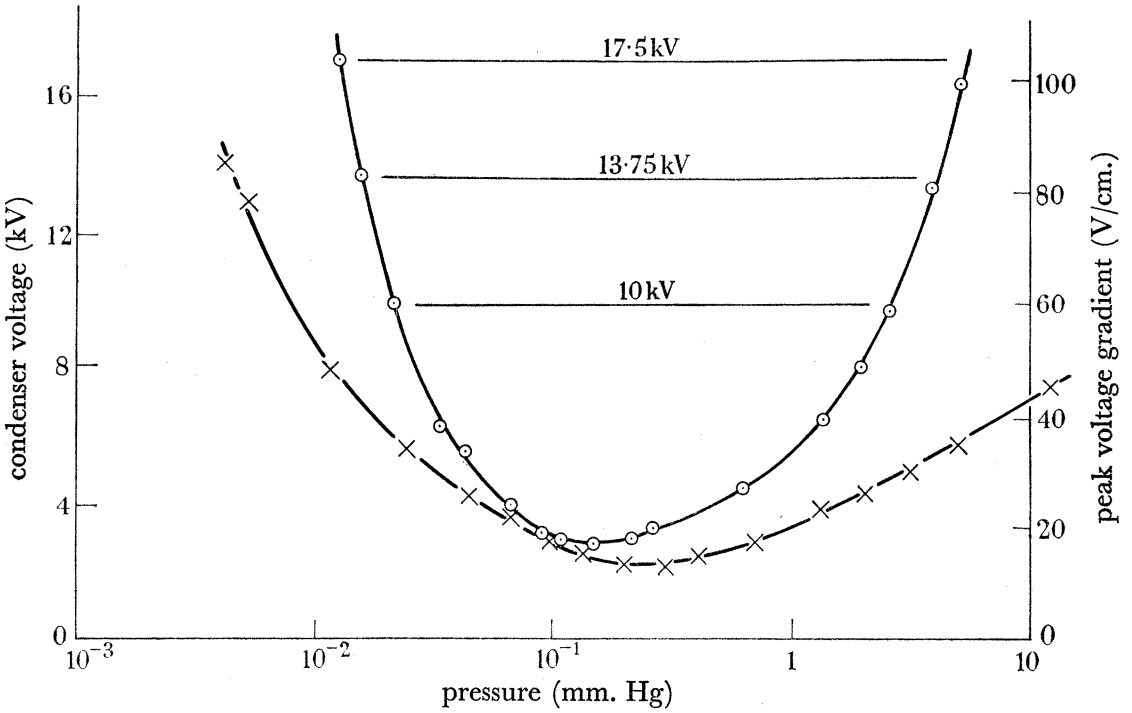

FIGURE 3. Variation of breakdown voltage with pressure: ⊙ hydrogen; × argon.

Provided the discharge was not repeated too frequently the breakdown voltages were found to repeat fairly consistently. But for this consistency it was necessary that some of the light from the spark gap should fall on the gas in the discharge tube. As is seen from figure 2 the spark gap *S* was situated very close to the torus, and it was possible for light which came out through the ventilation holes of the spark-gap box to be reflected on to the torus. If this light was blacked out the discharge became very inconsistent. Often a discharge would fail to occur even when the condenser voltage was several times the previous minimum breakdown potential. This need for a small amount of initial ionization so as to produce consistent results is typical of the measurement of sparking potentials in general (Loeb 1939).

The breakdown voltages were also measured for a torus which had only a 1 cm. feed-point gap in the copper, instead of the usual 1·8 cm. No difference in the breakdown voltages was detected.

In the work to be described here the condensers were charged to potentials considerably above the breakdown voltages. Three fixed voltages were used (10, 13·75 and 17·5 kV), and the variations of certain properties with change of pressure were studied. At these voltages an extremely intense discharge is produced, a very bright glow filling the torus and extending 6 in. or more into the side-arms. In hydrogen at the higher pressures (above about 0·5 mm.) the discharge is a very bright red in colour. At low pressures the discharge remains red at the inspection window and in the side-arms, but at the feed-point gap the discharge becomes white. In argon the discharge is dazzlingly bright, being comparable with the discharge flash lamps used in photography. The discharge is bluish white in colour at all pressures. At the

highest pressures a yellowish white afterglow is observed for several seconds after the flash. In both gases the light is most intense near the upper limit of pressure, and the intensity decreases steadily with decrease in pressure.

The appearance of the discharge can be seen from figures 9 to 12, plate 2, which shows photographs taken of the inspection window and the feed-point gap. With hydrogen the light intensity is fairly uniformly distributed across the tube at the inspection window, but at the feed-point gap the discharge is concentrated at the inside edge of the torus. This concentration becomes more marked as the pressure is decreased.

In argon the light at the inspection window is brighter at the inside edge of the tube at high pressures, but at medium and low pressures there is a concentration of the discharge at the centre of the tube. This bright central band decreases in width as the pressure is decreased. At the feed-point gap the discharge is concentrated towards the inside edge only at medium pressures. At high and low pressures the discharge is fairly uniform over the tube.

4. Cathode-ray oscillograms

Waveforms studied

The waveforms of three voltages connected with the discharge were studied. First, a voltage proportional to dI_1/dt (where I_1 is current in the copper coating) was obtained by tapping off part of one of the leads to one of the condensers. If k is the inductance of the length of lead then

$$V_1 = \frac{k}{4}\frac{dI_1}{dt}. \tag{1}$$

Secondly, a small pick-up loop was placed at the centre of the torus and co-axial with it. If m_1 and m_2 are mutual inductances of the loop with the copper coating and the gas respectively, then this second voltage is given by

$$V_2 = m_1\frac{dI_1}{dt} + m_2\frac{dI_2}{dt}, \tag{2}$$

where I_2 is the current in the gas.

These voltages were fed directly to the oscilloscope by means of co-axial cables which were matched at the oscilloscope by their characteristic impedance of 72 ohms. The use of low-impedance cable was permissible because of the very low impedance of the circuit being studied. As a result, the frequency response of the oscilloscope was extremely good; only at frequencies above 100 Mc./sec. does the capacity of the Y plate to earth become comparable with 72 ohms.

Thirdly, V_1 was applied to the Y_1 plate and V_2 to the Y_2 plate of the oscilloscope simultaneously. When no current passed in the gas (atmospheric pressure in the torus), the V_1 voltage was adjusted in amplitude so that it just balanced out the V_2 voltage. Then from equations (1) and (2), since $I_2 = 0$,

$$\frac{k}{4}\frac{dI_1}{dt} = m_1\frac{dI_1}{dt} \quad \text{or} \quad \frac{k}{4} = m_1.$$

If now a current passes in the gas the voltage developed between the Y_1 and Y_2 plates is

$$V_2 - V_1 = m_2\frac{dI_2}{dt} = V_3, \quad \text{say.} \tag{3}$$

Hence the voltage waveform V_3 is proportional to the rate of change of current in the gas. So as to obtain the gas current a series of the V_3 waveforms have been integrated graphically. Since the radius of cross-section of the gas is small compared with the radius of the torus, the magnetic field at the centre of the torus will be approximately $2\pi I_2/R$, and hence the mutual inductance between the gas and the pick-up loop m_2 is $2\pi^2 r^2/R$. (Correspondingly, m_1, the mutual inductance between the copper coating and the pick-up loop, is given by the same quantity and is therefore equal to m_2.) Using this value of m_2 the absolute values of the gas current have been calculated.

Description of oscillograms

(*a*) *Oscillograms for no gas current*

The V_1 and V_2 waveforms are identical when there is no gas current, and it is seen from figure 15, plate 3 that they are simple damped cosine waves. By comparison with the calibration trace (figure 17) the frequency of the oscillations is found to be 143 kc./sec. By measuring the damping the resistance of the condenser discharge circuit was found to be 0·05 ohm. The V_3 waveform for no gas current is shown in figure 16, plate 3. It was not found possible to balance the V_1 and V_2 waveforms exactly so as to obtain a perfectly straight trace. There was probably a small phase difference between V_1 and V_2 owing to the four condensers and their leads not being identical.

(*b*) *Oscillograms with gaseous currents flowing*

Examples of the V_1, V_2 and V_3 waveforms for hydrogen and argon at the condenser voltage 13·75 kV are shown in figures 18 to 20, plate 3. (The V_2 and V_3 waveforms have been photographed on the same oscillogram for comparison.) The actual gas-current waveforms (integrated V_3 waveforms) are shown in figure 4. The chief characteristics of the oscillograms are the following:

(i) The V_1 and V_2 oscillograms are considerably more damped when a gaseous discharge occurs. Also measurement of the wave-lengths shows that the frequency has increased by about 15 %. The frequency and damping ratio are shown plotted against pressure in figure 5, and from these readings the resistance of the gas is derived below.

(ii) From the V_3 and gas-current waveforms it is seen that near the limits of the pressure range the gas current does not become appreciable until several microseconds after the start of the condenser discharge. For convenience the point at which the gas current becomes measurable will be called the 'breakdown point'. At low pressures, as the pressure is decreased this point gradually occurs later in the first quarter-cycle and then jumps to the second half-cycle. It gradually occurs later in the second half-cycle and then jumps to the third half-cycle and so on. 'Breakdown points' as late as the fifth or sixth half-cycle have been observed. The ripple in the V_3 waveform up to the breakdown point is that due to the V_1 and V_2 voltages not being exactly balanced for zero gas current. For a given pressure the position of the 'breakdown point' remained constant, no statistical time lag being observed. (This, of course, was provided the light from the spark gap was allowed to play on the torus.) At low pressures dI_2/dt increases rapidly with time at the breakdown point so that this point is clearly defined on the waveforms, but at high pressures dI_2/dt increases slowly and there is no

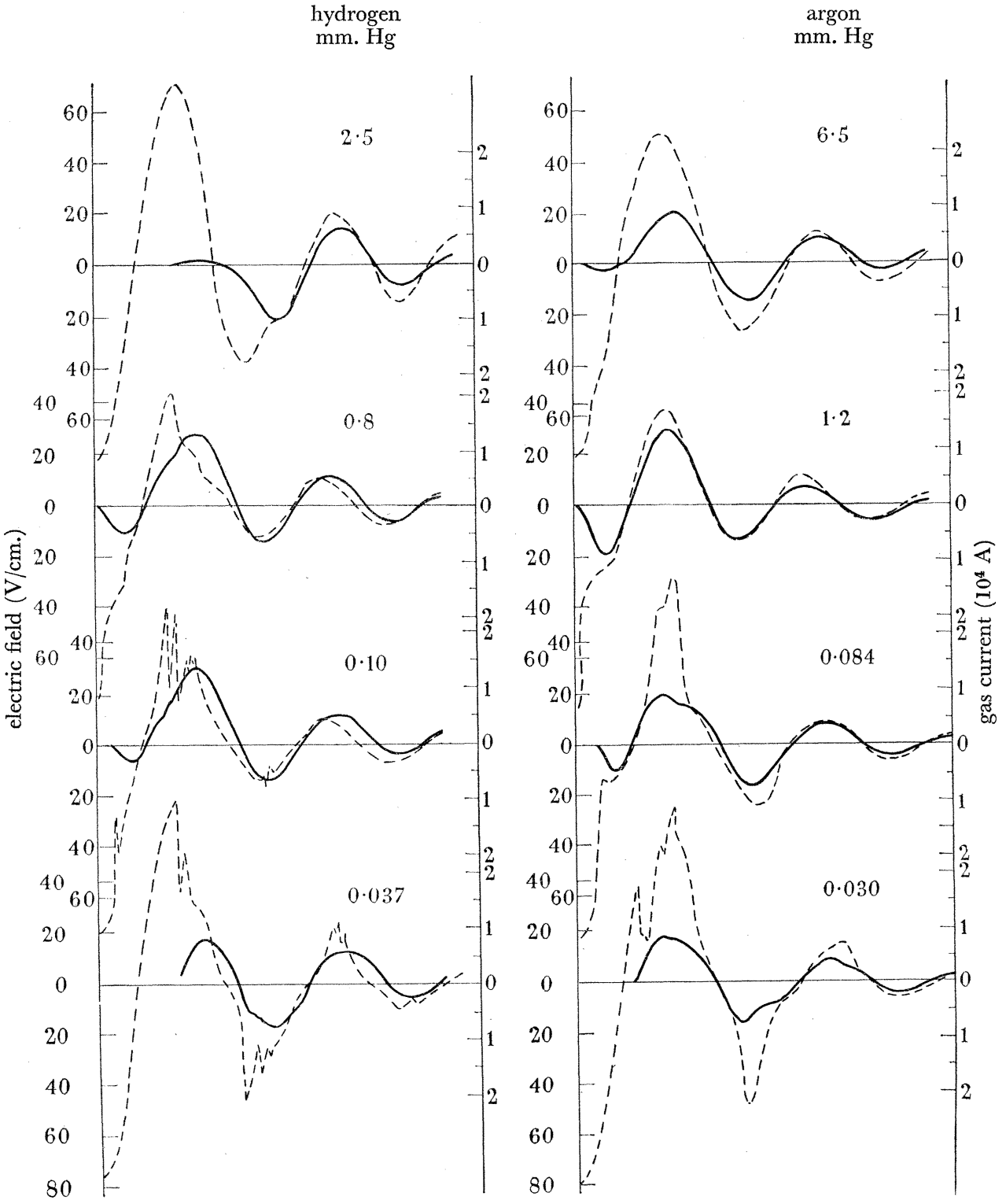

FIGURE 4. Electric field and gas current waveforms for the condenser voltage 13·75 kV: – – – electric field; —— gas current.

PHILOSOPHICAL TRANSACTIONS OF THE ROYAL SOCIETY A MATHEMATICAL, PHYSICAL & ENGINEERING SCIENCES

distinct breakdown point. (For example, see oscillograms shown in figure 19*a* and *d*, plate 3, which show high and low pressures respectively.)

(iii) The induced currents are extremely large; peak currents of the order of 15,000 A pass in the gas. The waveforms for the three different condenser voltages studied with hydrogen are similar in shape, their amplitude being approximately proportional to the voltage except that for pressures away from the centre of the range the breakdown point occurs sooner for a higher voltage. (Because of this similarity examples for only one voltage are shown.) In

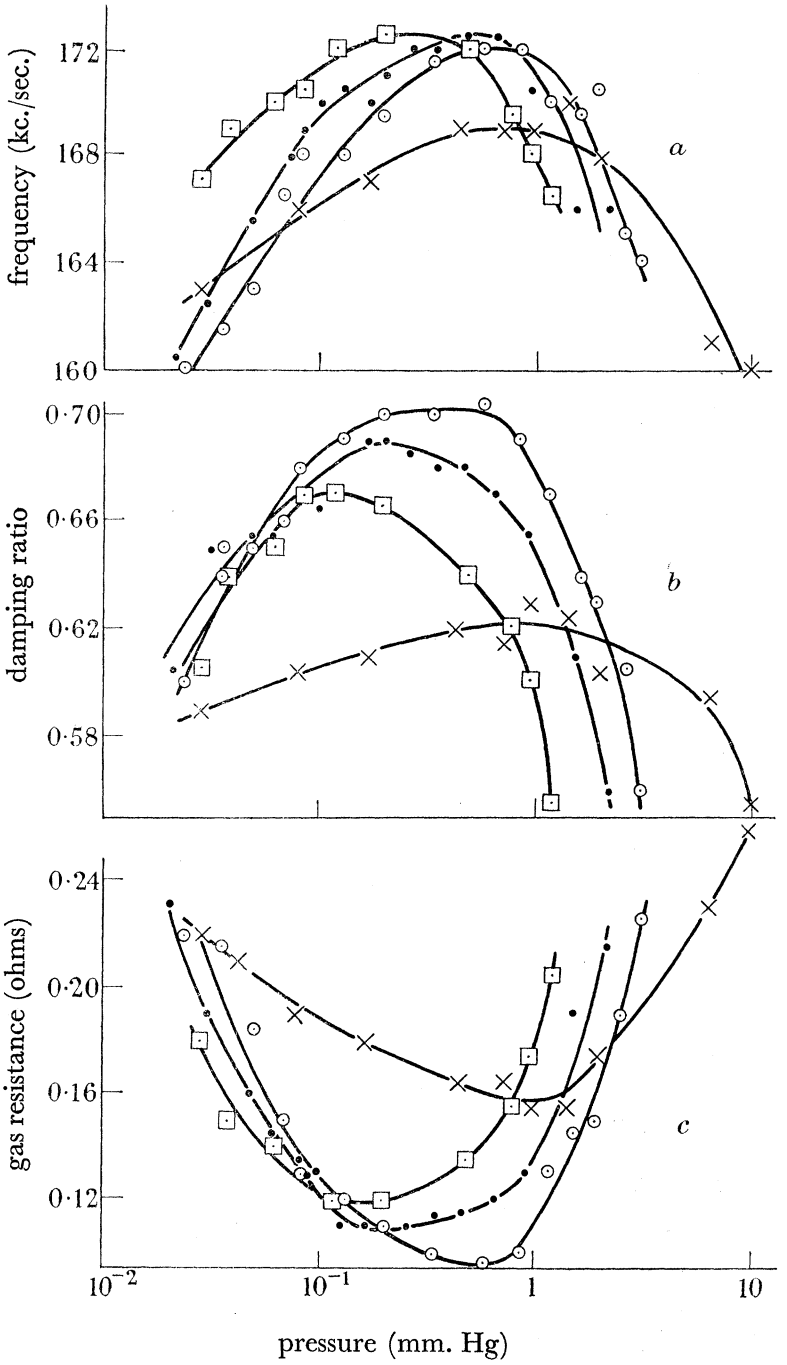

FIGURE 5. Variation of frequency, damping and gas resistance with pressure: ⊡, ●, ⊙ hydrogen, 10, 13·75 and 17·5 kV respectively; × argon, 13·75 kV.

argon the breakdown point occurs sooner than in hydrogen for the same pressure, and the build-up of current after breakdown is more rapid.

(In some cases the gas-current waveforms are seen to be asymmetrical about the zero current axis towards the end of the trace. This is thought to be due to errors in the integration rather than a real asymmetry in the current waveforms. Such an error may be that due to the V_1 and V_2 voltages not being completely matched for zero gas current, and there is also a possibility of error in estimating the initial sharp front of the V_3 waveforms.)

(iv) Lastly, a most noticeable feature of the oscillograms is that whereas at high pressures the waveforms retain a damped sine-wave appearance, at medium and low pressures the waveforms show a considerable number of irregularities. At medium pressures a single kink is observed in the second half-cycle, and as the pressure is lowered this kink develops into a series of oscillations. At the same time oscillations appear in other parts of the waveform. These oscillations, which will be referred to as the 'high-frequency oscillations' to distinguish them from the main oscillations, have been studied and their properties are described below.

Potential gradient in the gas

The e.m.f. acting in the gas when no gaseous currents are flowing is $M\frac{dI_1}{dt}$, where M is the mutual inductance between the metal coating and the gas. After breakdown the e.m.f. will be $M\frac{dI_1}{dt}+L_2\frac{dI_2}{dt}$, where L_2 is the self-inductance of the gas. Hence the potential gradient in the gas will be given by

$$E=\frac{1}{2\pi R}\left(M\frac{dI_1}{dt}+L_2\frac{dI_2}{dt}\right). \tag{4}$$

If the assumption is made that the gaseous currents are uniformly distributed over the cross-section of the discharge tube, then using the formula for a solid ring, L_2 is found to be $0{\cdot}38\mu$H for the torus used. Since it was found experimentally that there is no appreciable magnetic field within the torus (due to the screening effect of the copper), the inductance of the copper coating is merely that due to the field outside the torus. For the torus used this is $0{\cdot}315\mu$H. Lastly, since the flux linking the gas due to a current in the copper is exactly equal to the flux linking the copper coating itself, it follows that M is equal to the self-inductance of the copper.

Equation (4) can be rewritten in the form

$$E=\frac{M}{2\pi R}\left\{\left(\frac{dI_1}{dt}+\frac{dI_2}{dt}\right)+\frac{L_2-M}{M}\frac{dI_2}{dt}\right\}.$$

Hence if the V_1 and V_2 waveforms are added in the proportion $V_2+\left\{\frac{L_2-M}{M}\right\}V_3$, since $m_1=m_2$, a waveform is obtained which is proportional to the potential gradient in the gas. These waveforms have been constructed and are the broken-line curves in figure 4.

It is seen that the potential gradient waveforms are, as expected, very similar to the V_2 waveforms. Comparison with the current waveforms shows that the gas current is practically in phase with the electric field. The small lag of the current behind the electric field which is observed in some cases is almost certainly due to using too small a value for the self-inductance of the gas when deriving the electric field waveforms. If the currents in the gas are not

uniformly distributed over the discharge tube the self-inductance will be larger than the value taken. In deriving the potential gradient a larger fraction of the V_3 waveforms should therefore be added, and this will bring the waveforms into phase with that of the gas current. The photographs of the discharge do show a non-uniform distribution of the discharge, and as will be seen later, a concentration of the discharge at the centre of the tube is expected theoretically.

Average resistance of the gas

If the gas is assumed to behave as a simple ohmic resistance then the equivalent circuit is that shown in figure 6, where C is the capacity of the condensers, L_1 and R_1 the inductance and resistance of the primary circuit, L_2 and R_2 the inductance and resistance of the gas, and M the mutual inductance. The differential equation for the circuit is

$$(L_1L_2-M^2)\frac{d^3I}{dt^3}+(L_1R_2+L_2R_1)\frac{d^2I}{dt^2}+(R_1R_2+L_2S)\frac{dI}{dt}+R_2S=0, \tag{5}$$

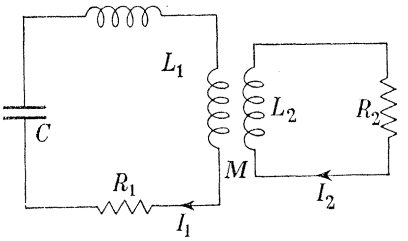

FIGURE 6

where S is $1/C$. If the circuit is less than critically damped the currents are of the form

$$I=Ae^{-qt}+Be^{-\beta t}\cos(\omega t+\theta), \tag{6}$$

where $-q$, $(-\beta\pm i\omega)$ are the roots of the auxiliary equation and A, B and θ are constants.

Since the auxiliary equation must be identical with the equation

$$(x+q)(x+\beta-i\omega)(x+\beta+i\omega)=0, \tag{7}$$

the coefficients can be equated, and by eliminating q and $(L_1L_2-M^2)$ the following relation is obtained:

$$R_2=\frac{(\omega^2+\beta^2)^2L_2R_1-2\beta(\omega^2+\beta^2)L_2S}{S(\omega^2-3\beta^2)-(\omega^2+\beta^2)^2L_1+2\beta(\omega^2+\beta^2)R_1}. \tag{8}$$

The constants R_1, S, L_1 and L_2 are all known, and the quantities ω and β can be obtained from the frequency and the damping decrement. Hence the resistance of the gas can be calculated from the observed readings. Figure 5*c* shows the gas resistance plotted against pressure.

The irregular waveforms for the gas current show that the gas does not in fact behave as a simple ohmic resistance, and hence the values obtained above must be regarded as the average resistance of the gas for the two cycles after breakdown, which was the region over which the measurements were made. It is seen that the curves of resistance against pressure are similar to the breakdown voltage curves. The minimum resistance, however, occurs at a higher pressure than the minimum breakdown potential. For the three different voltages in hydrogen it is seen that whereas at high pressures the resistance decreases with increase

PHILOSOPHICAL TRANSACTIONS OF THE ROYAL SOCIETY A MATHEMATICAL, PHYSICAL & ENGINEERING SCIENCES

in voltage, at low pressures the opposite seems to be the case. The point of minimum resistance occurs at a higher pressure when the voltage is increased. For argon the minimum resistance is considerably larger than with hydrogen and occurs at a higher pressure.

The high-frequency oscillations

The frequencies of the oscillations have been determined by measuring the wave-lengths between the peaks. At the high pressures where only a single kink is observed it is only possible to make a rough estimate of the wave-length, and where several oscillations are observed there is often a large difference between succeeding oscillations. Despite the fluctuations in individual readings, however, the mean period for a fixed pressure is fairly constant. Figure 7 shows the mean period plotted against pressure. The curves show a decrease in period with decrease in pressure except at the lowest pressures with hydrogen where the curves flatten out. There is a small difference between the readings for the three different voltages with hydrogen, the period decreasing with increase in voltage. The periods in argon are about three times the corresponding periods in hydrogen.

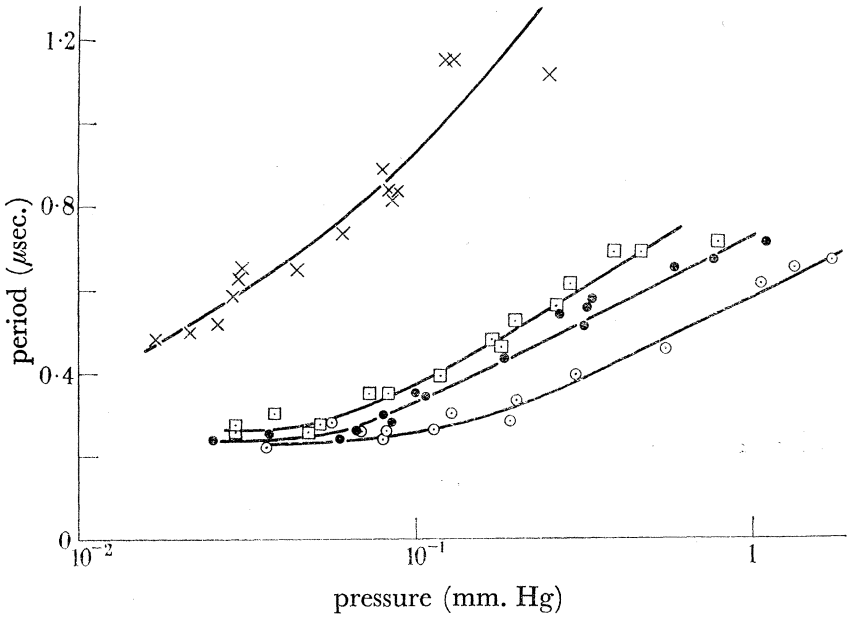

FIGURE 7. Variation of period of high-frequency oscillations with pressure: ⊡, ●, ⊙ hydrogen, 10, 13·75 and 17·5 kV respectively; × argon, 13·75 kV.

The oscillations occur mainly during the second half-cycle after breakdown. At low pressures oscillations occur in subsequent half-cycles but with diminishing amplitude. The oscillations do not occur continuously but in bursts at a particular part of each half-cycle. This is just after the gas current has passed through zero and while it is increasing. At high pressures the oscillations are regular and repeat themselves; at low pressures they are very irregular and vary from one oscillogram to another.

Photo-multiplier oscillograms

The light emitted from the inspection window and the feed-point gap was studied with the photo-multiplier. Examples of the oscillograms obtained are shown in plate 2. On each oscillogram the waveforms for different settings of the slit aperture were photographed. In

this way the variation of both the intense light and the initial faint light was studied. With the larger apertures the intense light saturates the photo-multiplier, and this causes the horizontal lines seen at the top of the oscillograms. The main points of interest shown by these oscillograms are as follows:

(1) At high pressures a small amount of light is always observed during the first quarter-cycle, although the corresponding current oscillograms show no measurable current in the gas until the second or third half-cycle. The light intensity increases slowly and takes several half-cycles to reach a maximum. At the low pressures, however, the oscillograms show no light emitted before the breakdown point even when the largest apertures are used. The light begins suddenly at a definite point and builds up very rapidly. This point coincides accurately with the 'breakdown point' observed on the corresponding current oscillogram.

(2) In hydrogen at high pressures the build-up of the light intensity is slow and the light does not reach a maximum until the fifth or sixth half-cycle, which is two or three half-cycles after the maximum current. As the pressure is decreased the light builds up more rapidly and the maximum intensity occurs nearer the peak current. At low pressure the maximum intensity occurs in the same half-cycle as the peak current. In argon the build-up of light intensity is much more rapid, and even at high pressures the maximum light occurs in the same half-cycle as the maximum current.

(3) After the first quarter-cycle the oscillograms for medium and high pressures (for both hydrogen and argon) show only a small variation of the light intensity with the main oscillations of the gas current. In hydrogen this variation is more marked at the feed-point gap than the inspection window. At low pressures there is a large variation of the light intensity with the oscillations of the current. These variations lag only a small amount behind the current oscillations.

(4) At the lowest pressures the oscillograms are irregular in shape; in some cases double peaks are observed in one half-cycle. These variations may be due to the high-frequency oscillations which were observed on the current waveforms. But because of the limited frequency response of the amplifier the true variation in the light due to these oscillations will not be detected.

5. Spectroscopic study

An initial study of the discharge spectra was made using a small quartz prism spectrograph. For this work a continuous stream of gas was passed through the torus and the discharge was fired with a repetition rate of about once every 3 sec. The condenser voltage used was 13·75 kV.

Hydrogen

(*a*) *Feed-point gap*

For pressures greater than about 1·5 mm. the spectrum consists of the Balmer lines, which are very broad, superimposed on a faint background of continuum. (The hydrogen molecular spectrum is very faint.) The continuum occurs over the whole spectrum range but is brightest near the limit of the Balmer series. As the pressure is decreased the lines become sharper and less intense and also the continuum becomes fainter. On the other hand, new spectral lines start to appear which are due to elements from the glass. At about 1 mm. pressure lines are

observed due to sodium and oxygen, and at 0·6 mm. silicon and boron lines also appear. As the pressure is decreased these new lines increase in intensity, whereas the hydrogen lines become fainter. At pressures below 0·2 mm. the hydrogen lines have completely disappeared.

(*b*) *Inspection window*

The spectrum emitted at the inspection window does not show the marked change with pressure observed at the feed-point gap. The Balmer lines do not disappear at low pressures but remain the most predominant in the spectrum. They do, however, show the increased sharpness with decrease in pressure. The spectral lines of the constituents of the glass are observed only for pressures below about 0·3 mm. and are very much fainter than in the case of the feed-point gap.

Argon

With argon in the torus the spectra observed for different pressures remained consistently the spectrum of argon. Even at low pressures no lines of the constituents of the glass were observed. Argon shows a brighter continuum than hydrogen, and at the highest pressures it is of considerable intensity.

Broadening of the Balmer lines

In order to make a more detailed study of the broadening of the Balmer lines the spectra were photographed again using an instrument of greater dispersion. This was a prism grating spectrograph with a dispersion of 250 Å/cm. of plate. From the spectral plates the contours of the H_β and H_γ lines were obtained by means of a recording microphotometer.

In order to calibrate the plates the spectrum for each pressure was photographed a number of times on the same plate for different exposure times, i.e. different numbers of flashes of the discharge. The intensities at the peaks of the H_β and H_γ lines were measured on the microphotometer and curves plotted of the microphotometer reading against exposure time. A reciprocity law was now assumed, and these graphs were taken as the intensity calibration curves. (To check this assumption the wedge slit method of calibration was also used on one plate. The two calibrations gave identical line profiles.) Examples of line profiles are shown in figure 8*a*. A correction was made for the continuum by taking the intensity level of this background as the zero intensity for the line profiles.

Determination of the ion concentration

Of the various causes of broadening of spectral lines, by far the most predominant in a highly ionized plasma in hydrogen is that due to the interatomic Stark effect (Finkelnburg 1931; Margenau & Watson 1936; and others). The theory of this type of broadening was derived by Holtsmark (1919), and recently it has been further developed by Craggs & Hopwood (1947) to determine the ion concentrations in spark channels in hydrogen. Holtsmark determined the probability function for the electric field at a point in an ionized plasma, and from this Craggs & Hopwood calculated the expected line contours for the Balmer lines H_α, H_β and H_γ. The breadths of the contours are proportional to F_n, the mean field strength, which, from Holtsmark's theory, is proportional to $N^{\frac{2}{3}}$, where N is the ion concentration. Hence by fitting the calculated contours to the observed line profiles, the scaling factor necessary on the wave-number axis will give the value of F_n and therefore the ion concentration.

The theory does not apply to the undisturbed radiation at the centre of the line profiles, because the undisplaced Stark components have not been taken into account. In addition, if the gas is excited intermittently by pulses of current, then the central undisturbed radiation will include all the light emitted when the ion concentration is decreasing during the recombination period. The calculated curves are fitted to the skirts of the observed profiles, and as a result it is the peak ion concentration which is measured.

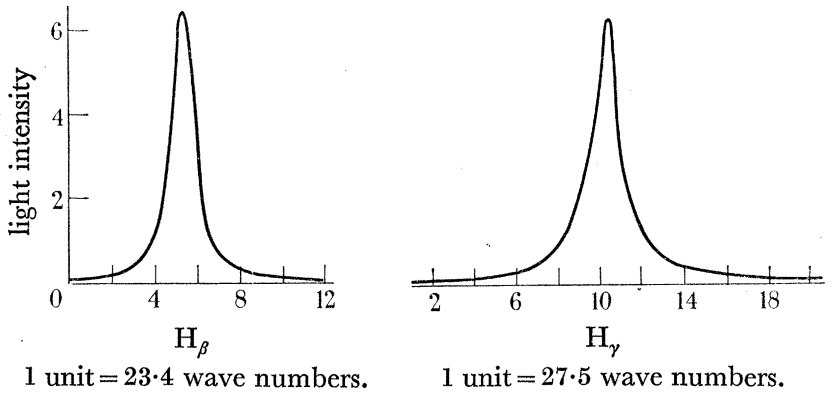

1 unit = 23·4 wave numbers. 1 unit = 27·5 wave numbers.

FIGURE 8*a*. Observed line profiles for pressure 0·6 mm. Hg.

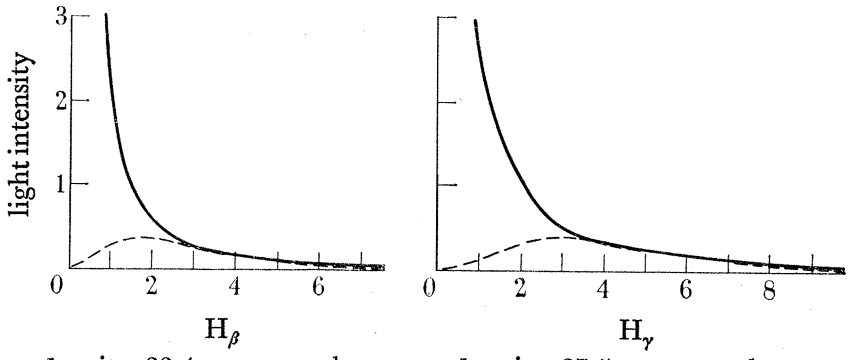

1 unit = 23·4 wave numbers. 1 unit = 27·5 wave numbers.

FIGURE 8*b*. Examples of calculated curves fitted to observed profiles (0·6 mm. Hg): —— observed profiles; – – – calculated curves.

The calculated contours of Craggs & Hopwood have been used to determine the ion concentrations in the toroidal discharge. Examples of the calculated curves fitted to the observed profiles are shown in figure 8*b*. Both observed and calculated profiles are symmetrical about the undisturbed position, and for convenience only half the profiles have been plotted. The values of F_n for the best scaling factors and the corresponding values of N are given in table 1. (N includes both positive and negative ions.) The equivalent percentage ionizations are also given.

TABLE 1

pressure (mm. of mercury)	F_n (kV/cm.) H_β	F_n (kV/cm.) H_γ	F_n (kV/cm.) mean	ion concentration (N) $10^{16}\times$	percentage ionization	ionization energy required (joules)
2·6	110	100	105	13	36	77
1·5	95	85	90	10	47	60
0·6	70	60	65	6·7	80	40
0·3	40	35	37	2·9	70	17

Craggs & Hopwood were able to fit the calculated curves to a large part of their observed profiles, namely, for intensities up to about a third of the intensity at the centre of the line. This suggests that a large part of the light was emitted whilst the peak concentration existed. Since square current pulses were used this seems quite likely. But in the work done here it has been found possible to fit the calculated curves only to the very base of the observed profiles, namely, for intensities up to about a twelfth of the peak intensity. It would therefore seem that there is no predominant ion concentration, and that a large proportion of the light is emitted at ion concentrations below the maximum.

Craggs & Hopwood determined F_n to an accuracy of 10 %. In the work done here however, although it is possible to fit the curves to this accuracy, the value of F_n is not likely to be more accurate than 20 %. This is because the calculated curves have been fitted to the extreme base of the profiles where the microphotometer readings are least accurate. In determining the ion concentrations from the values of F_n the accuracy here depends on the validity of applying Holtsmark's theory. The simplifying assumption has been made that the electric field is constant over the dimensions of an atom, so that the theory for the simple Stark effect in a homogeneous field can be applied. The results obtained by Craggs & Hopwood agreed to within a factor of 2 with approximate calculations of the ion concentration made from the current, potential gradient and breadth of the spark channels. But a more accurate check than this has not been made on this method of determining the ion concentration.

6. Theoretical considerations

Breakdown of the gas

For the initiation of a ring discharge no secondary ionizing mechanism is necessary. The lines of current flow form closed paths and this acts as the secondary mechanism. (In the discharge studied here secondary processes will undoubtedly occur, but they are not likely to supply more than a small fraction of the total ionization.) Since the rate of recombination in the gas will be small at the low pressures used in ring discharges, the main loss of ions will be due to diffusion to the walls. Hence the condition for breakdown is that the rate of production of ions by electronic collisions should exceed the losses due to diffusion. In the case of a ring discharge excited by a train of damped oscillations an extra condition is necessary in that the 'breakdown time' (the time for the build-up of a measurable current) must be less than the duration of the exciting voltage.

In the discharge studied here, at high pressure where the electron mean free path is very small compared with the cross-section of the discharge tube the rate of diffusion of ions to the walls will be small. The build-up of current will depend mainly on the rate at which the electrons can ionize. Since for a given pressure and electric field the value of the Townsend coefficient is considerably larger in argon than in hydrogen, a discharge will occur more easily in argon at high pressures.

At low pressures where the mean free path is comparable with the cross-section of the discharge tube, the losses to the walls will become large and will greatly limit the rate of increase of ionization. Because the mean free path is shorter in argon than in hydrogen the losses due to diffusion will be less. Also the larger cross-section for ionization in argon will

be important, since electrons will undergo only a few collisions in the gas before reaching the walls. Hence at low pressures as well, a discharge will occur more easily in argon.

It is seen from the V_3 waveforms that the breakdown process at low pressures is very slow at first, but at a critical point it suddenly becomes cataclysmic. Since the sudden change cannot be due to an increase in the rate at which the electrons can ionize it must be due to a reduction in the diffusion losses. Such an effect will occur when a sufficient number of electrons have reached the walls to cause an appreciable wall potential. When the potential becomes comparable with the energy of the electrons there will be a sudden reduction in the diffusion losses, and this will lead to the rapid breakdown observed. Prior to this point the losses to the walls will be very large and the rate of ionization will be very slow.

The 'electrostatic' field

At the feed-point gap in addition to the induced field there will be an 'electrostatic' field caused by the large voltage difference between the ends of the metal coating. The magnitude of this field will depend on the proportion of lines of force between the ends of the coating which pass through the glass and invade the gas. Since the voltage across the gap is equal to the total induced e.m.f. in the gas round the whole circumference, this 'electrostatic' field will be considerably larger than the induced field. To determine whether this field plays any appreciable part in the breakdown, the following experiment was carried out. A short length of glass tubing of the same diameter as that used to make the torus was placed alongside the feed-point gap and connected to the vacuum system. Sleeve electrodes were fitted round the tube at the same distance apart as the gap on the torus. These electrodes were connected to the terminals of the torus. With atmospheric pressure in the torus the condensers were discharged in the usual manner so that the voltage across the feed-point gap was applied to the sleeve electrodes. Although a wide range of pressures was tried in the tube no visible discharge was observed.

Workers who have studied the discharges produced by such sleeve electrodes (J. Thomson 1930, 1934 & 1937 and others) have produced glow discharges with voltages considerably less than those used here. But in none of the papers on this type of discharge is a frequency less than a megacycle quoted, and it seems likely that the frequency used here is too low to produce such an effect. This experiment thus leads to the conclusion that no appreciable amount of ionization is caused by the 'electrostatic' field. This is confirmed by the fact that the breakdown potentials were the same when a narrow feed-point gap was used.

After breakdown the highly ionized gas will be similar to a metallic conductor, and the magnitude of the field in the gas will depend on the capacitative coupling between the copper coating and the gas. A simple calculation shows that this capacity is of the order of 260 pF and its impedance to 150 kc./sec. is 4000 ohms. The resistance of the gas, however, was found to be of the order of 0·1 ohm. Since the peak voltage across the gap after breakdown is about 4000 V the voltage developed in the gas will be about a tenth of a volt and the current about an ampere. Such a current is negligible compared with the 10^4 A due to the ring discharge.

The discharge after breakdown

After breakdown the conditions in the gas will be very complex, and the following considerations are aimed merely at showing the general effects to be expected. Since the gas is

screened from external fields by the copper, the magnetic field at any point will be approximately the same as that in a straight cylinder of current of the same cross-section. When the gas current is 10,000 A the field will vary from zero at the centre of the tube to 1400 G at the perimeter. This large magnetic field will greatly affect the motion of the electrons in the gas.

Axes have been chosen at any point P in the gas such that the z axis is radial with respect to the discharge tube and the y axis parallel to the axis of the tubing. The induced electric field causing the discharge is in the direction of the y axis and the magnetic field at P will lie along the x axis. These fields will be denoted by Y and H respectively. If these were the only forces acting, then an electron at P would perform a trochoidal path inwards along the negative z axis. Taking collisions into account the resultant effect would be a transverse drift inwards, combined with a forward drift parallel to the electric field. Similarly, electrons at other parts of the gas will tend to move inwards to the axis of the discharge tube. But such a motion of the electrons will polarize the gas, since the positive ions will be left behind due to their slower mobility. Hence a radial space-charge force will be set up which will counteract the inward drift of the electrons. This field will be denoted by Z. A much slower inward drift of both electrons and positive ions will now occur depending on the mobility of the positive ions. This drift will at first be neglected so as to determine the magnitude of the space-charge force.

The components of the electron drift velocity in crossed electric and magnetic fields (Chapman & Cowling 1939) are

$$V_1 = \frac{Ee\tau}{m(1+\theta^2\tau^2)}, \tag{9}$$

$$V_2 = \frac{Ee\theta\tau^2}{m(1+\theta^2\tau^2)}, \tag{10}$$

where V_1 is the forward component parallel to the electric field E, and V_2 is the transverse component at right angles to both the electric and magnetic fields. τ is the mean collision interval, e and m are the charge and mass of the electron, and θ is equal to He/m.

Provided that the electron mean free path is small compared with the cross-section of the discharge tube then these expressions can be applied to give the drift velocities in the toroidal discharge. For there to be no resultant inward drift of the electrons the transverse drift due to Y must be balanced by the forward drift due to the space-charge field Z. Hence from equations (9) and (10)

$$\frac{Ye\theta\tau^2}{m(1+\theta^2\tau^2)} = \frac{Ze\tau}{m(1+\theta^2\tau^2)}.$$

Hence

$$Z = \theta\tau Y = \frac{HYe\tau}{m}. \tag{11}$$

Thus Z is proportional to both H and Y. It will therefore vary from zero at the centre of the tube to a maximum at the perimeter, and the variation with time will be given by

$$\exp(-2\beta t)\sin^2(\omega t).$$

The assumption has been made that the transverse diffusion forces are negligible compared with Z, and hence equation (11) only holds for the initial stages of the discharge before any appreciable constriction has occurred.

By means of equations (9) and (10) it is also possible to derive the drift velocity of the electrons in the y direction. This will be the sum of the forward drift due to Y and the transverse drift due to Z, i.e.

$$v = \frac{Ye\tau}{m(1+\theta^2\tau^2)} + \frac{Ze\theta\tau^2}{m(1+\theta^2\tau^2)}.$$

Substituting for Z from equation (13)

$$v = \frac{Ye\tau(1+\theta^2\tau^2)}{m(1+\theta^2\tau^2)} = \frac{Ye\tau}{m}. \tag{12}$$

Thus the resultant drift velocity parallel to the applied electric field is independent of H and Z and is therefore constant over the cross-section of the discharge tube. Its magnitude is the same as if neither H nor Z were present, since $e\tau/m$ is the normal mobility of an electron in an electric field.

The 'pinch' effect

The theory of the 'pinch' effect developed by Tonks (1939) shows that the currents observed here would be easily large enough to produce an appreciable 'pinch' if they were continuous. Whether a 'pinch' will be observed in the toroidal discharge, however, will depend on whether there is sufficient time for the contraction to take place. The space-charge force Z must be sufficiently large to cause an appreciable movement of the positive ions during the short duration of the discharge.

To estimate Z from equation (11) it is necessary to know the value of τ, the mean collision interval, which is approximately equal to the mean free path divided by the mean thermal velocity of the electrons. These quantities have been measured by Townsend (1948) and his co-workers in direct current discharges for low values of the parameter Y/p, the ratio of electric field to pressure. At high pressures in the discharge studied here the values of Y/p come within the range covered by Townsend, and although the conditions in the toroidal discharge are widely different from those studied by Townsend, it is proposed to use his values of τ for the approximate calculations carried out here. Thus at the pressure 3 mm. Hg the average value of Y/p for the first half-cycle after breakdown is about 10 V cm.$^{-1}$ mm.$^{-1}$, and the values of τ are $0{\cdot}9 \times 10^{-10}$ and $1{\cdot}5 \times 10^{-10}$ sec. in hydrogen and argon respectively. Since the current in the gas is of the order of 10^4 A the magnetic field at the edge of the discharge tube is 1400 G, and hence from equation (11) the values of Z at the edge of the tube are 40 and 70 V cm.$^{-1}$ in hydrogen and argon respectively. Only a very small movement of the electrons with respect to the positive ions is necessary to produce such fields. These fields will therefore develop very rapidly after breakdown.

To determine the movement of the positive ions caused by Z their mobility is assumed to be $eL/2MC$, where L, M and C are the mean free path, mass and mean thermal velocity of the ions. The positive ions in hydrogen are assumed to be protons and their mean free path to be the same as that of electrons. Kinetic theory mean free paths are used, and for the sake of this rough calculation the mean energy of the positive ions is assumed to be about half a volt in hydrogen and a tenth of a volt in argon; these are approximately the energies the positive ions can themselves gain from the electric field in a mean free path. Hence the mobilities are found to be $1{\cdot}3 \times 10^4$ and $4{\cdot}3 \times 10^2$ cm.^{2} sec.$^{-1}$ V^{-1} for hydrogen and argon respectively. The inward velocities of the positive ions at the edge of the discharge tube will

PHILOSOPHICAL TRANSACTIONS OF THE ROYAL SOCIETY A MATHEMATICAL, PHYSICAL & ENGINEERING SCIENCES

therefore be 5×10^5 and 3×10^4 cm.sec.$^{-1}$ respectively. Because of the damping Z will have dropped to less than half the above value by the second half-cycle, and hence the effective duration of Z is about half a cycle, i.e. 3 μsec.

The positive ions should therefore move about a centimetre in hydrogen but only about a millimetre in argon. A marked 'pinch' effect should therefore be observed in hydrogen at 3 mm. Hg. Also since τ increases with decrease in pressure and the positive-ion mobility becomes larger, a 'pinch' should be observed in hydrogen at all pressures, the effect developing more rapidly the lower the pressure.

Considering now argon at say 0·1 mm. Hg, if the mean energy of the electrons is assumed to be about 10 V and that of the positive ions 1 V, and if kinetic theory mean free paths are used, then Z is found to be 1000 V cm.$^{-1}$ and the velocity of the positive ions is 4×10^6 cm.sec.$^{-1}$. Thus although no 'pinch' effect should be observed in argon at high pressures, as the pressure is decreased a contraction of the current filament should gradually develop and should be very marked at low pressures.

Referring to the photographs of the discharge at the inspection window (figures 9 and 11, plate 2) it is seen that argon behaves as expected. At medium and low pressures the light shows a bright band at the centre of the discharge tube which gets narrower the lower the pressure. In hydrogen, however, although at high pressures there is a small falling off of intensity at the edges of the tube, at medium and low pressures the light is uniform across the tube.

(Very recently the discharge has been studied using a rotating mirror. Although the resolution is not very good the photographs suggest that a 'pinch' does occur in hydrogen, but that the thin current filament moves backwards and forwards across the discharge tube, making the resultant picture look uniform.)

Ion concentrations

From equation (12) it was seen that the electron drift velocity was constant over the cross-section of the discharge and equal to $Ye\tau/m$. Hence assuming a uniform electron concentration n throughout the torus, and since Y does not vary appreciably across the tube the current in gas is given by

$$I = \frac{\pi a^2 n e Y e \tau}{m},$$

and hence

$$n = \frac{mI}{\pi a^2 e^2 Y \tau}, \tag{13}$$

where a is the radius of cross-section of the discharge tube. Table 2 gives the peak gas currents and corresponding potential gradients which occur in the waveforms for hydrogen (condenser voltage 13·75 kV). The values of τ measured by Townsend are again used and are given in the fourth column of table 2. The ion concentrations obtained from equation (13) are given in the last column.

Comparing tables 1 and 2 it is seen that the spectroscopic values $\frac{1}{2}N$ are approximately 30 times larger than n. It must first be remembered that the spectroscopic method was such that the highest concentration existing in any part of the discharge will be the one measured, whereas n represents an average over the cross-section of the tube. Nevertheless, the two sets of values will be consistent only if there is a very large variation in the ion concentration over

the cross-section of the discharge tube, namely, if a very marked 'pinch' effect exists. The high spectroscopic values are therefore evidence in favour of a 'pinch' effect having occurred in hydrogen.

TABLE 2. CALCULATED ION CONCENTRATIONS FOR HYDROGEN

pressure (mm. Hg)	peak gas current (10^3 A)	potential gradient (V cm.$^{-1}$)	mean collision interval (τ) (10^{-10} sec.)	ion concentration (n)
2·5	10	22	1·0	$2{\cdot}6\times10^{15}$
1·9	10·5	22	1·3	$2{\cdot}1\times10^{15}$
0·77	13·1	20	2·6	$1{\cdot}1\times10^{15}$

That the high concentration $\frac{1}{2}N$ could not exist over the whole of the discharge tube can be seen by considering the energy required to produce such ionization. Since the volume of the gas in the torus is approximately 500 cm.^{3} the energy required is $500NE/2$ electron volts, where E is the ionization potential. The values of this quantity are given in the last column of table 1, where E has been taken as 15 V. (These figures represent the absolute minimum energy required to produce such ionization. In actual fact the average energy dissipated in producing an ion pair is probably at least 30 eV.) The energy stored by the condensers is 180 joules, and about two-thirds of this is dissipated in the gas, i.e. 120 joules. At the time of the peak gas current only about half the energy has been dissipated. There is thus a maximum of 60 joules available for ionization. It is thus clear that there is not sufficient energy available to produce such ionization throughout the whole volume of gas.

The discharge at the feed-point gap

The study of the light from the torus showed that the discharge at the feed point differs considerably from that at the inspection window. This effect must be caused by a difference in either the electric or magnetic fields occurring at these points after breakdown. The only extra electric field at the feed point is the 'electrostatic' field considered above, but since this field becomes negligibly small after breakdown it cannot be the cause of the observed differences.

Since at the feed-point gap there is no copper coating, all the external magnetic fields will invade the gas at this point. By far the largest field is that caused by the leads carrying the current to the torus. These leads are parallel and about 4 cm. long, and since they carry currents in opposite directions their magnetic fields will add for points between the two leads. For the peak current in the copper of 20,000 A the magnetic fields at the outside edge, the centre and the inside edge of the tube will be 2500, 700 and 200 G respectively. A study of the V_1 and V_3 waveforms shows that the current in the copper is very nearly 180° out of phase with the gas current. This magnetic field will therefore pass through zero at approximately the same time as the gas current, and the force on the current will always be in the same direction. This direction is towards the inner wall. Thus not only is there a much stronger magnetic field at the outside edge of the tube making it more difficult for a discharge to start there, but there is also a transverse force causing the electrons to drift towards the inner wall. Since the magnetic field is of the same order of magnitude as the self-field of the gas current, the arguments used with respect to the movement of positive ions in the 'pinch' effect will apply equally here. Hence a concentration of the discharge along the inner wall is expected in hydrogen at all pressures and in argon at medium and low pressures.

In this case the discharge in hydrogen does behave as expected. The photographs of the feed-point gap (figure 10, plate 2) show such a concentration towards the inner wall at all pressures. The effect is more marked the lower the pressure, as would be expected. Argon (figure 12) shows the concentration at medium pressures but not at low pressures where the discharge appears uniform. In hydrogen at low pressures the discharge is concentrated very close to the wall, and it must be this effect which results in greater heating and vaporization of the glass at this point, by causing increased bombardment.

The high-frequency oscillations

Since the frequency of these oscillations varies considerably with the nature and pressure of the gas in the torus, they cannot be due to a combination of inductance and capacity in the discharge or measuring circuits. The oscillations must be due to some mechanism in the gas itself such as plasma oscillations. Of these, since the frequency of plasma electron oscillations will be much greater than the observed frequencies, the only possibility is a plasma-ion oscillation, the frequency of which is given by (Tonks & Langmuir 1929)

$$\nu = \left(\frac{ne^2}{\pi M + \dfrac{ne^2 M \lambda^2}{\boldsymbol{k} T}} \right)^{\frac{1}{2}}, \tag{14}$$

where n is the ion concentration, M the mass of the ions, T the electron temperature, e the electronic charge, $\boldsymbol{k}$ Boltzmann's constant and λ the wave-length of the oscillations in the plasma. If λ^2 is small compared with $\pi \boldsymbol{k} T/ne^2$ the ions have a natural frequency given by $(ne^2/\pi M)^{\frac{1}{2}}$, but at the high ion concentrations in the torus this frequency is also much greater than the observed frequencies.

If λ^2 is large compared with $\pi \boldsymbol{k} T/ne^2$ then

$$\nu = \frac{1}{\lambda} \left(\frac{\boldsymbol{k} T}{M} \right)^{\frac{1}{2}}. \tag{15}$$

There is now no natural frequency for the ions. The waves are similar to sound waves, and from the analogy one would expect any natural frequency to depend on the dimensions of the discharge vessel. If the Townsend values of the electron temperatures are used the wave-lengths corresponding to the observed frequencies are of the order of a centimetre. This is comparable with the width of the discharge tube, and hence frequencies of the observed order of magnitude could be produced by lateral oscillations of the plasma. (The condition $\lambda^2 \gg \pi \boldsymbol{k} T/ne^2$ is satisfied, since for the assumed temperatures and an ion concentration of the order of 10^{15} per cm.^{3}, $\pi \boldsymbol{k} T/ne^2$ is of the order of 10^{-6} cm.^{2}.)

A likely form of oscillation is an alternate contraction and expansion of the current filament, which could be caused by the strong 'pinch' forces. Such oscillations will be expected to occur while the current is building up and while it is large, i.e. when the 'pinch' is taking place. This agrees with the position of the observed oscillations. The observed increases in frequency with decrease in pressure and increase in voltage are expected from equation (15), since both will lead to a higher electron temperature. The ratio of the frequencies in hydrogen and argon should be given by

$$\frac{\nu_{\mathrm{H}}}{\nu_{\mathrm{A}}} = \left(\frac{T_{\mathrm{H}} M_{\mathrm{A}}}{T_{\mathrm{A}} M_{\mathrm{H}}} \right)^{\frac{1}{2}} = 6{\cdot}3 \left(\frac{T_{\mathrm{H}}}{T_{\mathrm{A}}} \right)^{\frac{1}{2}}, \tag{16}$$

where M_H and M_A are the masses of the ions in the two gases and T_H and T_A the respective electron temperatures.

When the Y/p value is 15 (the highest value studied in argon by Townsend's co-workers), the ratio of the electron temperatures in hydrogen and argon is 0·2. This gives the ratio of the frequencies to be 2·8, which is in good agreement with the observed ratio of 3. But the Y/p values for the pressures at which the high-frequency oscillations have been observed are considerably greater than 15, and since the ratio of the temperatures is increasing with Y/p, the agreement would probably not be so good if the correct temperatures were known.

The theory of Tonks & Langmuir assumes a simple uniform plasma in which the electric field is small and where the electrons are in thermal equilibrium. In the torus there are not only large electric fields but also large magnetic fields and the electrons will not be in thermal equilibrium. Hence the simple plasma theory cannot be expected to describe accurately the observed oscillations.

Operation as an induction accelerator

The magnetic field within the torus due to the gas current varies from a large positive value at the outside edge of the tube to a large negative value at the inside edge, where a positive field bends the electron paths in the same direction as the curvature of the torus. For most of the cycle these fields are considerably larger than those linking the torus, and hence somewhere between the mean radius of the torus and the outside radius there will be a radius r_0 where the field is half the average field linking the torus, i.e. where the betatron condition is satisfied. The conditions for stability of the betatron orbit, namely, that the magnetic field must decrease with radius less rapidly than $1/r$ and the lines of force must be convex outwards, are well satisfied over the outside half of the discharge tube. The magnetic field actually increases with r, and the lines of force are very convex. Hence if it is possible for fast electrons to exist in the gas and behave as if they were in a vacuum, then the discharge will act as induction accelerator similar to the betatron.

The above magnetic field, however, is not the only one acting in the gas. At the feed point there is the very large positive field due to the current leads. Also the field due to the gas current which is concentrated along the inside wall will be positive over most of the tube. Hence the two fields will add and will prevent electrons from circulating the torus even once, since electrons with as much as several thousand volts energy will have their paths bent into the wall by this strong field. (As expected, experiments showed no X-rays produced by the discharge.)

If the current leads can be suitably designed to eliminate this disturbing field, then the question as to whether the discharge will act as an induction accelerator will depend on whether a group of fast electrons can develop in the gas and behave as if they are in a vacuum. Since very little is known about the conditions in a highly ionized gas, this question can only be answered experimentally.

The author is indebted to Professor Sir George P. Thomson for his suggestion of this problem, and for his general guidance and many valuable discussions throughout the work.

PHILOSOPHICAL TRANSACTIONS OF THE ROYAL SOCIETY A MATHEMATICAL, PHYSICAL & ENGINEERING SCIENCES

References

Chapman, S. & Cowling, T. G. 1939 *The mathematical theory of non-uniform gases*, p. 335. Cambridge University Press.

Craggs, J. D., Haine, M. E. & Meek, J. M. 1946 *J. Instn Elect. Engrs*, **93**, IIIA, 191, 963.

Craggs, J. D. & Hopwood, W. 1947 *Proc. Phys. Soc.* **59**, 755.

Esclangon, F. 1934 *Ann. Phys., Paris*, **1**, 276.

Finkelnburg, W. 1931 *Z. Phys.* **70**, 375.

Holtsmark, J. 1919 *Ann. Phys., Lpz.*, **58**, 577.

Knipp, C. T. & Knipp, J. K. 1931 *Phys. Rev.* **38**, 948.

Kunz, J. 1932 *Phil. Mag.* **13**, 964.

Loeb, L. B. 1939 *Fundamental processes of discharge in gases*, p. 459. New York: John Wiley.

Margenau, H. & Watson, W. W. 1936 *Rev. Mod. Phys.* **8**, 22.

Smith, C. G. 1941 *Phys. Rev.* **59**, 997.

Smith, C. G. 1947 *Phys. Rev.* **71**, 135.

Steenbeck, M. & Hoffmann, K. 1943 *Siemens Technical Report* HW/PL, No. 27 (13 December).

Thomson, J. 1930 *Phil. Mag.* **10**, 280.

Thomson, J. 1934 *Phil. Mag.* **18**, 686.

Thomson, J. 1937 *Phil. Mag.* **23**, 1.

Thomson, Sir J. J. 1927 *Phil. Mag.* **4**, 1128.

Thomson, Sir J. J. 1928 *Proc. Phys. Soc.* **40**, 79.

Tonks, L. 1939 *Phys. Rev.* **56**, 360.

Tonks, L. & Langmuir, I. 1929 *Phys. Rev.* **33**, 195.

Townsend, Sir John 1948 *Electrons in gases*, p. 71. London: Hutchinson.

Tykocinski-Tykociner, S. 1932 *Phil. Mag.* **13**, 953.

Wasserrab, T. Z. 1946 Harwell, EM/H, 307.

PHILOSOPHICAL TRANSACTIONS OF THE ROYAL SOCIETY A MATHEMATICAL, PHYSICAL & ENGINEERING SCIENCES

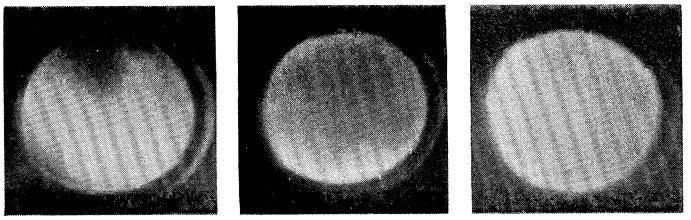

a. 1·9 mm. Hg *b*. 0·4 mm. Hg *c*. 0·10 mm. Hg

FIGURE 9. Photographs of inspection window, hydrogen.

a. 2·0 mm. Hg *b*. 0·1 mm. Hg *c*. 0·02 mm. Hg

FIGURE 10. Photographs of feed-point gap, hydrogen.

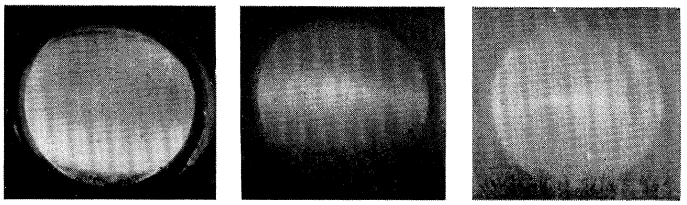

a. 2·1 mm. Hg *b*. 0·25 mm. Hg *c*. 0·02 mm. Hg

FIGURE 11. Photographs of inspection window, argon.

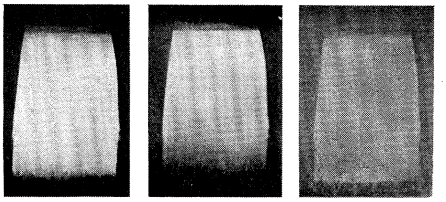

a. 1·0 mm. Hg *b*. 0·23 mm. Hg *c*. 0·026 mm. Hg

FIGURE 12. Photographs of feed-point gap, argon.

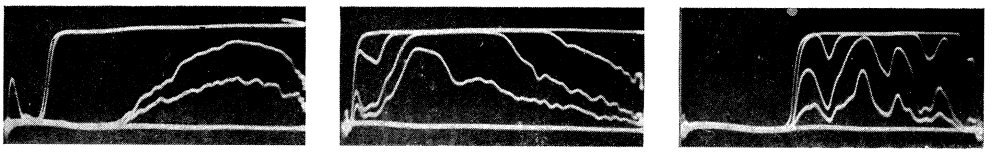

a. 2·5 mm. Hg *b*. 0·10 mm. Hg *c*. 0·017 mm. Hg

FIGURE 13. Photo-multiplier oscillograms; hydrogen, condenser voltage 13·75 kV.

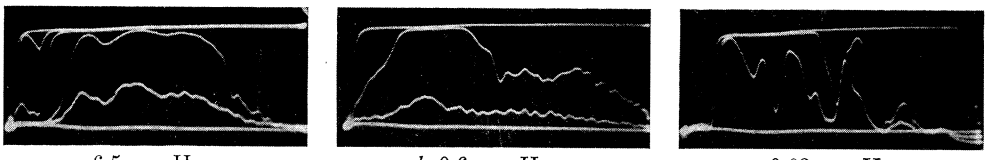

a. 6·5 mm. Hg *b*. 0·6 mm. Hg *c*. 0·03 mm. Hg

FIGURE 14. Photo-multiplier oscillograms; argon, condenser voltage 13·75 kV. (The same time base was used as for oscillograms on plate 3.)

(*Facing p.* 220)

PHILOSOPHICAL TRANSACTIONS OF THE ROYAL SOCIETY A MATHEMATICAL, PHYSICAL & ENGINEERING SCIENCES

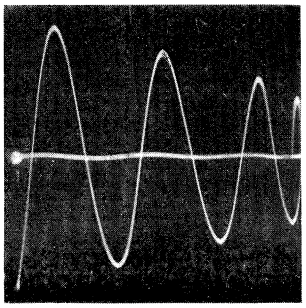

FIGURE 15. $V_1 = dI_1/dt$; no gas current.

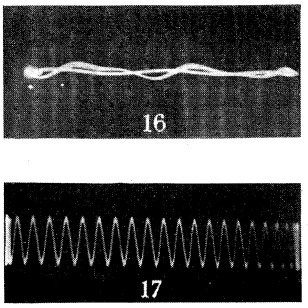

FIGURE 16. V_3; no gas current.

FIGURE 17. Time base calibration. (1 Mc./sec.)

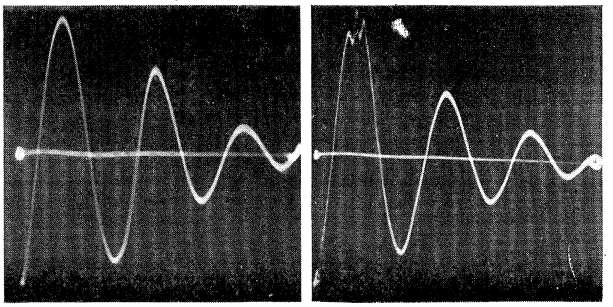

a. 2·2 mm. Hg *b*. 0·10 mm. Hg

FIGURE 18. V_1 waveforms, hydrogen.

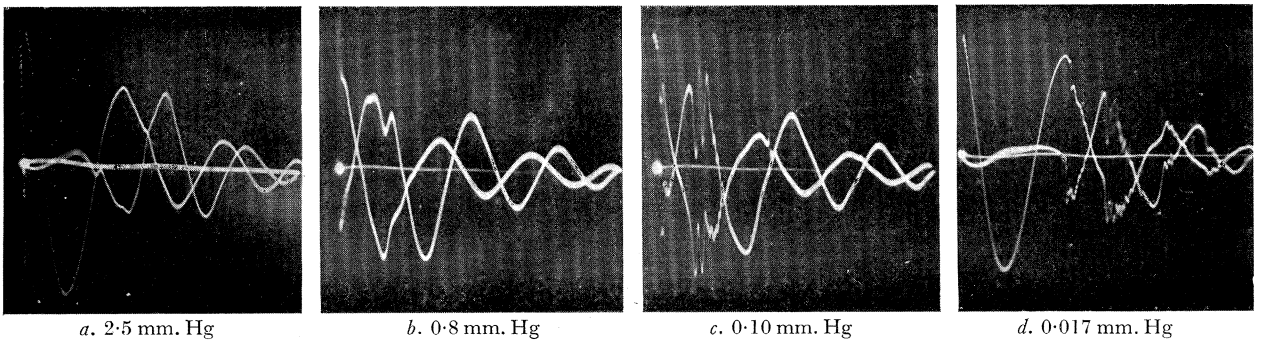

a. 2·5 mm. Hg *b*. 0·8 mm. Hg *c*. 0·10 mm. Hg *d*. 0·017 mm. Hg

FIGURE 19. V_2 and V_3 waveforms, hydrogen.

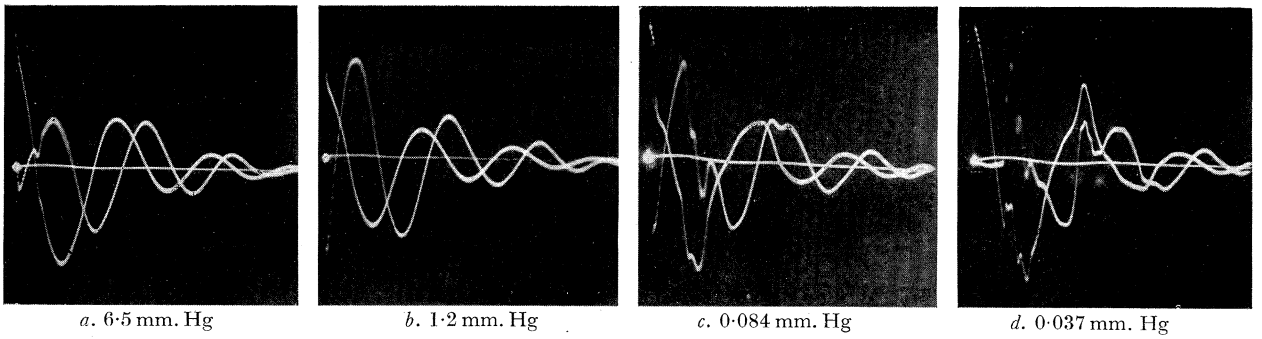

a. 6·5 mm. Hg *b*. 1·2 mm. Hg *c*. 0·084 mm. Hg *d*. 0·037 mm. Hg

FIGURE 20. V_2 and V_3 waveforms, argon.

(The V_2 waveforms are those starting with large positive deflexions.)
All oscillograms are for the condenser voltage 13·75 kV.

PHILOSOPHICAL TRANSACTIONS OF THE ROYAL SOCIETY A MATHEMATICAL, PHYSICAL & ENGINEERING SCIENCES

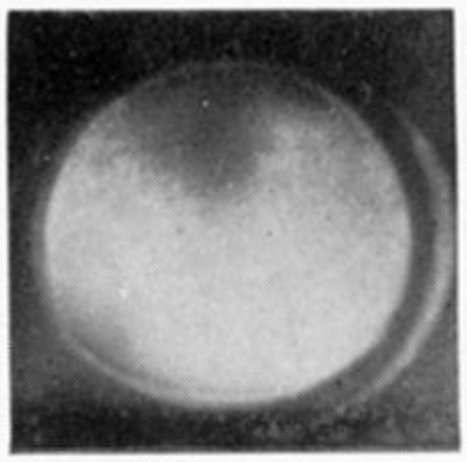

a. 1·9 mm. Hg

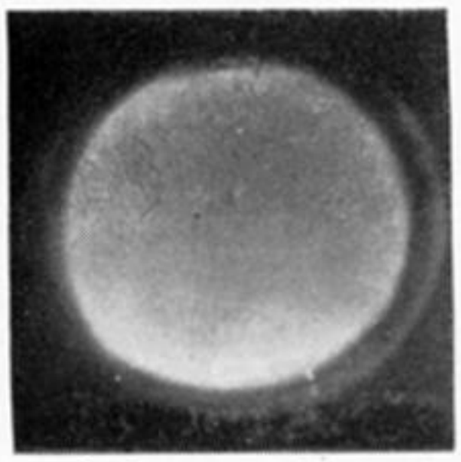

b. 0·4 mm. Hg

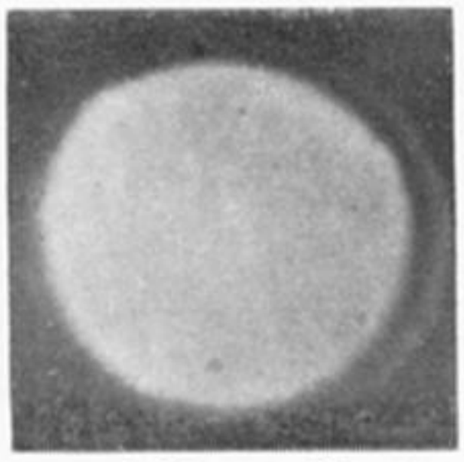

c. 0·10 mm. Hg

FIGURE 9. Photographs of inspection window, hydrogen.

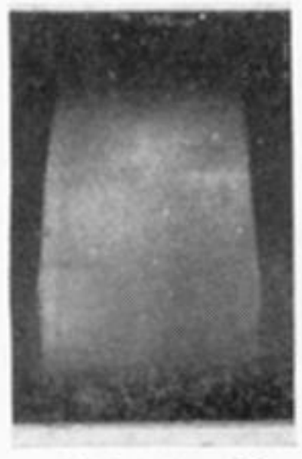

a. 2·0 mm. Hg

b. 0·1 mm. Hg

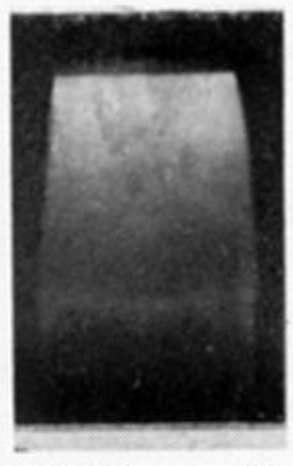

c. 0·02 mm. Hg

FIGURE 10. Photographs of feed-point gap, hydrogen.

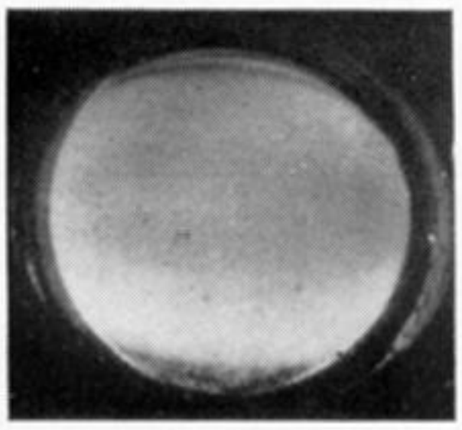

a. 2·1 mm. Hg

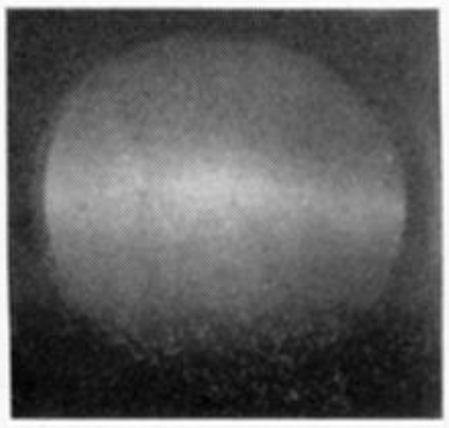

b. 0·25 mm. Hg

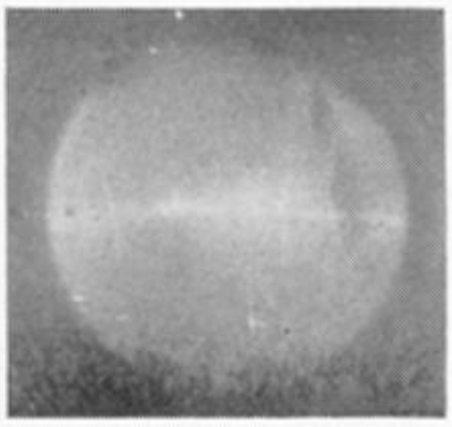

c. 0·02 mm. Hg

FIGURE 11. Photographs of inspection window, argon.

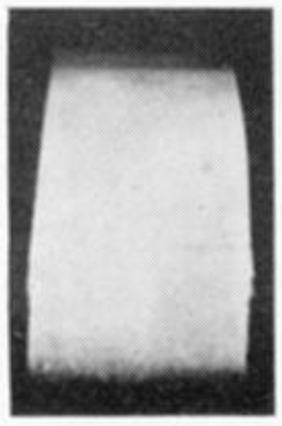

a. 1·0 mm. Hg

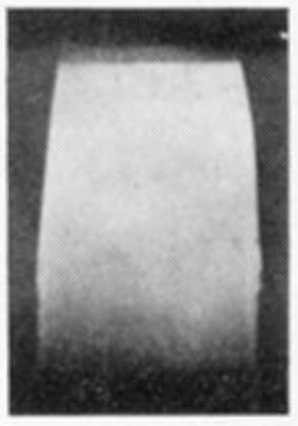

b. 0·23 mm. Hg

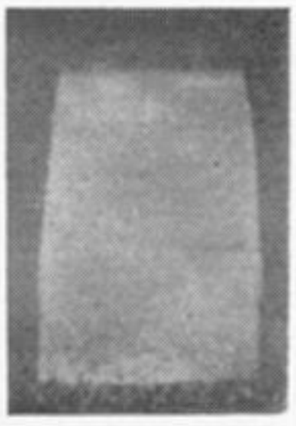

c. 0·026 mm. Hg

FIGURE 12. Photographs of feed-point gap, argon.

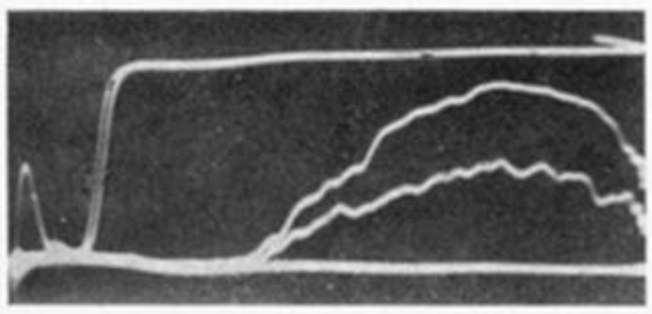

a. 2·5 mm. Hg

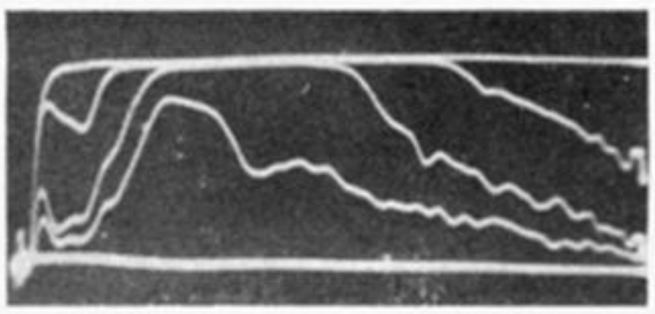

b. 0·10 mm. Hg

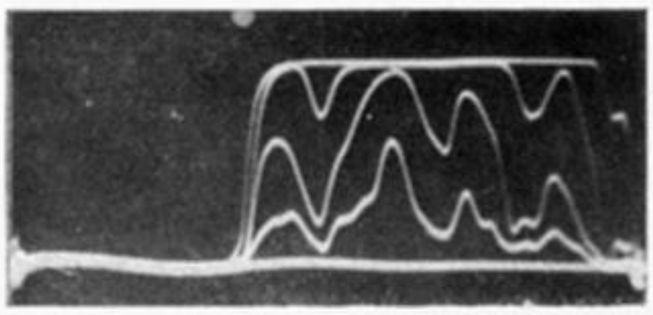

c. 0·017 mm. Hg

FIGURE 13. Photo-multiplier oscillograms; hydrogen, condenser voltage 13·75 kV.

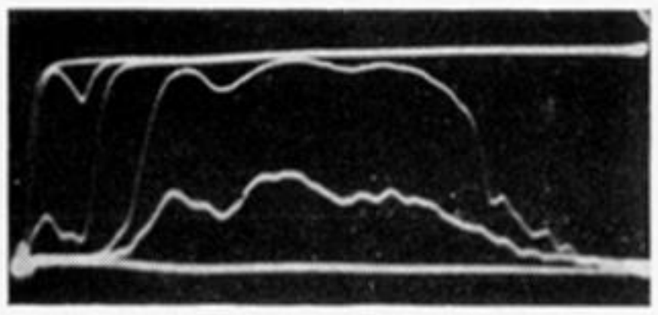

a. 6·5 mm. Hg

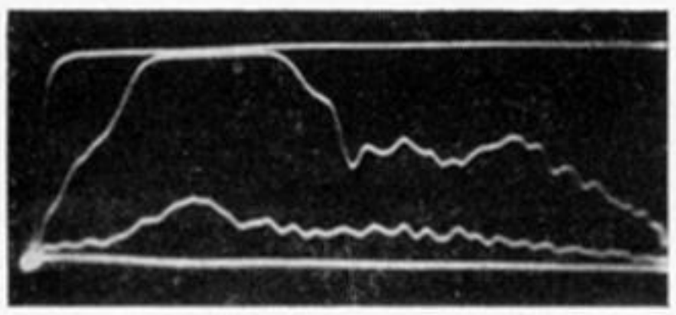

b. 0·6 mm. Hg

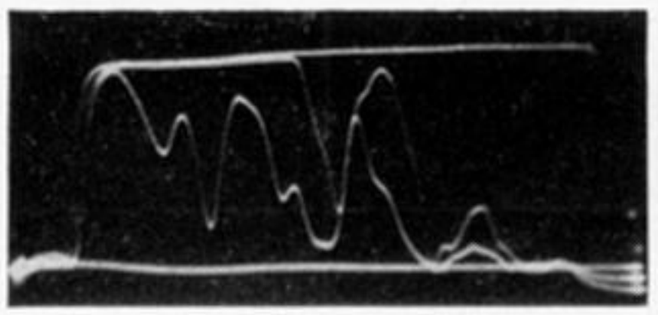

c. 0·03 mm. Hg

FIGURE 14. Photo-multiplier oscillograms; argon, condenser voltage 13·75 kV.
(The same time base was used as for oscillograms on plate 3.)

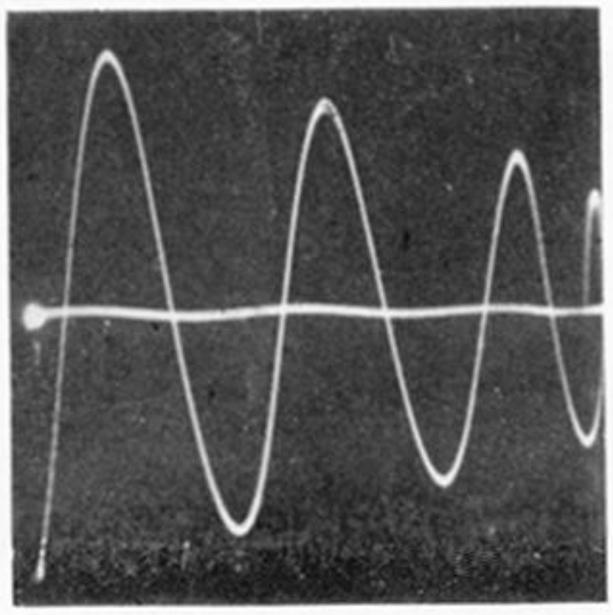

FIGURE 15. $V_1 = dI_1/dt$; no gas current.

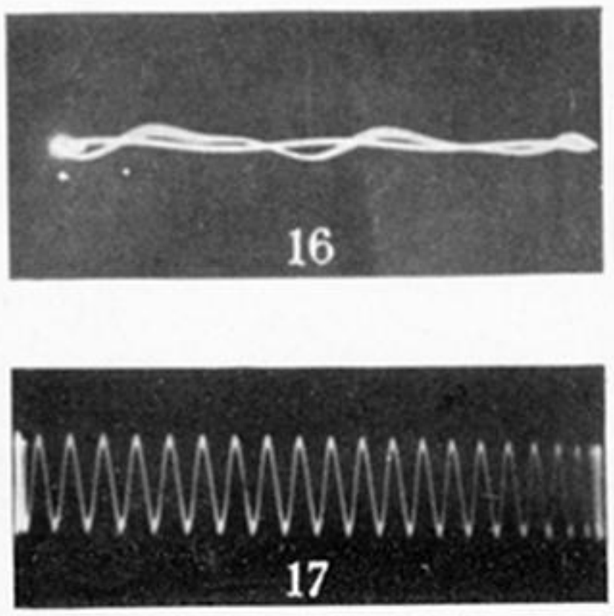

FIGURE 16. V_3; no gas current.

FIGURE 17. Time base calibration. (1 Mc./sec.)

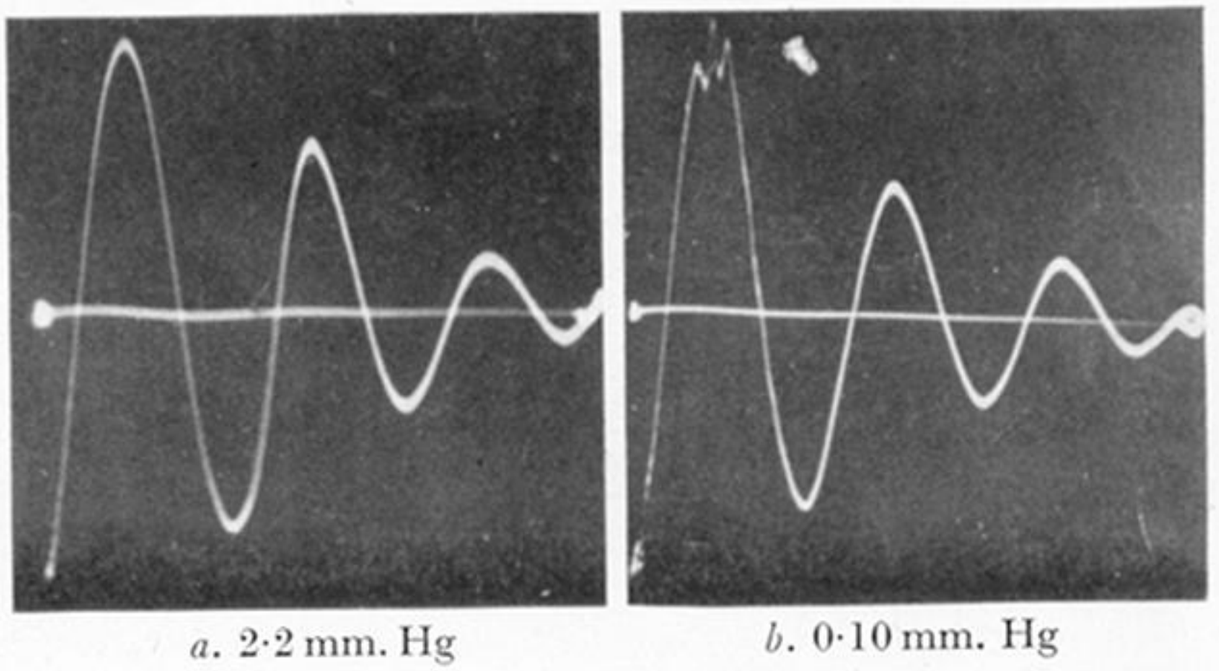

a. 2·2 mm. Hg *b*. 0·10 mm. Hg

FIGURE 18. V_1 waveforms, hydrogen.

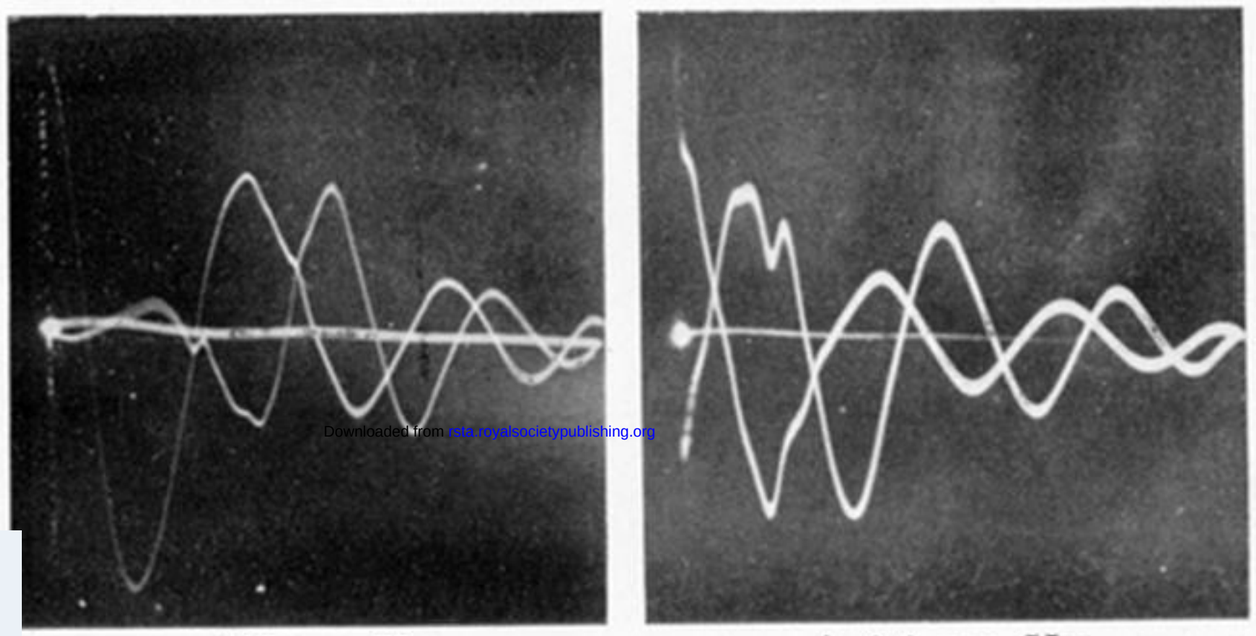

a. 2·5 mm. Hg *b*. 0·8 mm. Hg *c*. 0·10 mm. Hg *d*. 0·017 mm. Hg

FIGURE 19. V_2 and V_3 waveforms, hydrogen.

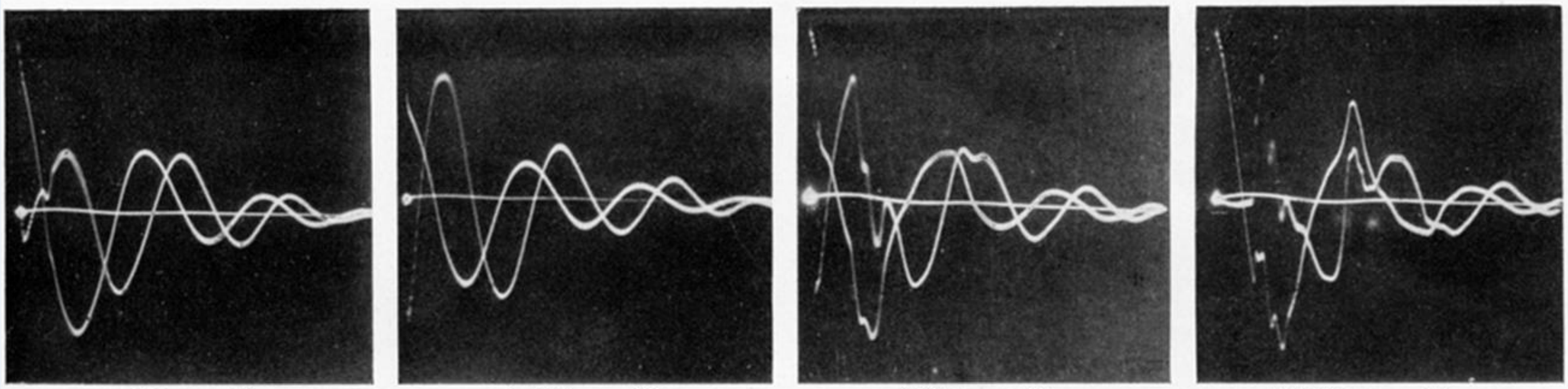

a. 6·5 mm. Hg *b*. 1·2 mm. Hg *c*. 0·084 mm. Hg *d*. 0·037 mm. Hg

FIGURE 20. V_2 and V_3 waveforms, argon.

(The V_2 waveforms are those starting with large positive deflexions.)
All oscillograms are for the condenser voltage 13·75 kV.